



OH regeneration from methacrolein oxidation investigated in the atmosphere simulation chamber SAPHIR

H. Fuchs¹, I.-H. Acir¹, B. Bohn¹, T. Brauers¹, H.-P. Dorn¹, R. Häsel¹, A. Hofzumahaus¹, F. Holland¹, M. Kaminski¹, X. Li¹, K. Lu^{1,*}, A. Lutz², S. Nehr^{1,**}, F. Rohrer¹, R. Tillmann¹, R. Wegener¹, and A. Wahner¹

¹Institute of Energy and Climate Research, IEK-8: Troposphere, Forschungszentrum Jülich GmbH, Jülich, Germany

²Institute of Chemistry and molecular Biology, Göteborg University, Gothenburg, Sweden

* now at: College of Environmental Sciences and Engineering, Peking University, Beijing, China

** now at: Verein Deutscher Ingenieure e.V., Kommission Reinhaltung der Luft, Düsseldorf, Germany

Correspondence to: H. Fuchs (h.fuchs@fz-juelich.de)

Received: 24 January 2014 – Published in Atmos. Chem. Phys. Discuss.: 25 February 2014

Revised: 26 June 2014 – Accepted: 27 June 2014 – Published: 8 August 2014

Abstract. Hydroxyl radicals (OH) are the most important reagent for the oxidation of trace gases in the atmosphere. OH concentrations measured during recent field campaigns in isoprene-rich environments were unexpectedly large. A number of studies showed that unimolecular reactions of organic peroxy radicals (RO₂) formed in the initial reaction step of isoprene with OH play an important role for the OH budget in the atmosphere at low mixing ratios of nitrogen monoxide (NO) of less than 100 pptv. It has also been suggested that similar reactions potentially play an important role for RO₂ from other compounds. Here, we investigate the oxidation of methacrolein (MACR), one major oxidation product of isoprene, by OH in experiments in the simulation chamber SAPHIR under controlled atmospheric conditions. The experiments show that measured OH concentrations are approximately 50 % larger than calculated by the Master Chemical Mechanism (MCM) for conditions of the experiments (NO mixing ratio of 90 pptv). The analysis of the OH budget reveals an OH source that is not accounted for in MCM, which is correlated with the production rate of RO₂ radicals from MACR. In order to balance the measured OH destruction rate, 0.77 OH radicals (1σ error: ±0.31) need to be additionally reformed from each reaction of OH with MACR. The strong correlation of the missing OH source with the production of RO₂ radicals is consistent with the concept of OH formation from unimolecular isomerization and decomposition reactions of RO₂. The comparison of observations with model calculations gives a lower limit of 0.03 s⁻¹ for the reaction rate constant if the OH source is at-

tributed to an isomerization reaction of MACR-1-OH-2-OO and MACR-2-OH-2-OO formed in the MACR + OH reaction as suggested in the literature (Crouse et al., 2012). This fast isomerization reaction would be a competitor to the reaction of this RO₂ species with a minimum of 150 pptv NO. The isomerization reaction would be the dominant reaction pathway for this specific RO₂ radical in forested regions, where NO mixing ratios are typically much smaller.

1 Introduction

Isoprene (2-methyl-1,3-butadiene) is the most abundant non-methane hydrocarbon emitted by the biosphere and predominantly removed by oxidation with atmospheric hydroxyl radicals (OH) (Guenther et al., 2012). Unexpectedly large OH concentrations that cannot be explained by the current knowledge of atmospheric chemistry have been found in several field campaigns (Carslaw et al., 2001; Tan et al., 2001; Kuhn et al., 2007; Ren et al., 2008; Lelieveld et al., 2008; Hofzumahaus et al., 2009; Lu et al., 2012, 2013; Stone et al., 2010; Whalley et al., 2011; Wolfe et al., 2011) for high loads of OH reactants (often dominated by isoprene) and low concentrations of nitrogen monoxide (NO). As a potential explanation for the high OH concentrations, reformation of OH radicals from unimolecular reactions of organic peroxy radicals (RO₂) that result from the reaction of isoprene with OH has been suggested (Peeters et al., 2009; Peeters and Müller, 2010; da Silva et al., 2010). The proposed reactions involve

1,5-H- and 1,6-H-shift reactions followed by decomposition of specific isoprene RO₂ isomers and compete with the well-known OH reformation via reaction of HO₂ with NO. This reaction scheme has been applied in order to explain high levels of OH radicals, using reaction rate constants that were derived from quantum chemical calculations (Peeters et al., 2009; Taraborrelli et al., 2012). A laboratory study investigated the product yields of the proposed reactions (Crouse et al., 2011; Wolfe et al., 2012), and direct OH measurements in experiments in the atmosphere simulation chamber SAPHIR gave evidence for OH regeneration from isoprene RO₂ without involvement of NO (Fuchs et al., 2013). Results from these experimental studies are consistent with the RO₂ isomerization reaction scheme, but also showed that isomerization reaction rate constants are smaller than those calculated by Peeters and Müller (2010). Thus, OH regeneration from isoprene peroxy radicals alone cannot explain elevated OH concentrations found in field campaigns. Therefore, the question arises of whether unimolecular RO₂ reactions from the oxidation products of isoprene may also enhance atmospheric OH.

Methacrolein (2-methylpropenal) is one of the major first-generation products of the gas-phase oxidation of isoprene by OH with a yield of approximately 20–30% for atmospheric conditions (Tuazon and Atkinson, 1990; Galloway et al., 2011; Liu et al., 2013). Methacrolein (MACR) is further oxidized by OH in the atmosphere, producing hydroxyacetone, methylglyoxal, and formaldehyde (Galloway et al., 2011). Similar unimolecular reactions of RO₂ as for isoprene, which may produce additional OH, have also been suggested for MACR (Peeters et al., 2009; Crouse et al., 2012; Asatryan et al., 2010; da Silva, 2012). Recently, the product distribution from the MACR plus OH reaction for various NO concentrations has been investigated in a laboratory study accompanied by quantum chemical calculations (Crouse et al., 2012). The authors of that study inferred a new reaction pathway in which hydroxyacetone is formed independently of the level of NO. This would be consistent with a fast unimolecular RO₂ reaction, because hydroxyacetone has so far only been known as a product of the reaction of RO₂ with NO. The new reaction path is attributed to a 1,4-H-shift isomerization reaction with concurrent reformation of OH confirmed by isotopic measurements reported in the work by Crouse et al. (2012).

Here, we present the investigation of the photooxidation of MACR by OH at controlled atmospheric conditions in the simulation chamber SAPHIR in the presence of approximately 90 pptv NO. Measurements allow for a detailed analysis of the OH budget. Recently proposed reaction pathways are tested by comparing time series of measurements with model calculations.

2 Methods

2.1 Simulation experiment in SAPHIR

Experiments were conducted in the atmosphere simulation chamber SAPHIR in Jülich, Germany. The chamber allows for the investigation of the photochemical oxidation of organic compounds at atmospheric conditions with respect to temperature, pressure, radiation, and concentrations of trace gases and radicals. Experiments for this study were similar to those that were performed to investigate the oxidation of isoprene by OH (Fuchs et al., 2013).

The outdoor SAPHIR chamber is made of a double-wall Teflon (FEP) film of cylindrical shape (length 18 m, diameter 5 m, volume 270 m³). Details of the chamber can be found elsewhere (Rohrer et al., 2005; Bohn et al., 2005; Schlosser et al., 2009). It is equipped with a shutter system which can be opened to expose the chamber air to natural sunlight. The FEP film has a high transmittance for the entire spectrum of solar radiation (Bohn et al., 2005). Slight overpressure prevents leakage of ambient air into the chamber. The chamber air is mixed from evaporated liquid nitrogen and oxygen of highest purity (Linde, purity > 99.99990%). During all experiments reported here, a fan ensured fast mixing of the chamber air (mixing time < 2 min). Replenishment of chamber air, which is lost due to small leakages and consumption by instruments, leads to a dilution of trace gases at a rate of approximately 4% h⁻¹.

The chamber experiments aimed to simulate conditions like those found during several field experiments (Lu et al., 2012, 2013) in which unexpectedly large OH concentrations were measured. At the beginning of the experiment, the dark chamber only contained clean synthetic air. The water vapour mixing ratio was increased by flushing water vapour from boiling Milli-Q[®] water into the chamber in the dark until the relative humidity reached approximately 80%. Then the shutter system was opened to expose the chamber to sunlight. Ozone produced from a silent discharge ozonizer (O3Onia) was added, resulting in a mixing ratio of approximately 50 ppbv. The initial phase (“ZA”) with zero air, water vapour, and ozone had a total duration of 2 h. Thereafter, MACR was injected several times, increasing the mixing ratio by 7 ppbv each time. The maximum mixing ratio was 14 ppbv. The experiment was performed three times in a similar way (Table 1). On 11 August 2011 OH production rates from photolysis were highest and a large number of instruments was available. Therefore, time series and model calculations from this experiment are shown here. Experiments on the other two days give similar results and are included in the analysis of the OH budget.

The major primary source for OH in the chamber is photolysis of nitrous acid (HONO), which is released from the Teflon film depending on temperature, relative humidity, and strength of radiation (Rohrer et al., 2005). HONO photolysis is also the major source of nitrogen oxides. In addition,

Table 1. Experimental conditions of the MACR oxidation experiments. Maximum values are given for MACR, and averaged values are given for the part of the experiment when MACR was present for the other parameters.

MACR ppbv	OH 10^6 cm^{-3}	NO _x ppbv	NO pptv	O ₃ ppbv	RH %	$j(\text{NO}_2)$ 10^{-3} s^{-1}	T K	Date
14	2.5	0.8	90	40	40	4	301	11 Aug 2011
7	3.5	0.7	60	50	30	4	308	29 Aug 2012
9	3.5	0.6	70	40	45	4.5	302	6 Sep 2012

Table 2. Instrumentation for radical and trace gas detection during the MACR oxidation experiments.

	Technique/instrument	Time resolution	1σ precision	1σ accuracy
OH	DOAS ^a (Dorn et al., 1995; Hausmann et al., 1997; Schlosser et al., 2007)	205 s	$0.8 \times 10^6 \text{ cm}^{-3}$	6.5 %
OH	LIF ^b (Lu et al., 2012)	47 s	$0.3 \times 10^6 \text{ cm}^{-3}$	13 %
HO ₂ , RO ₂	LIF ^b (Fuchs et al., 2011)	47 s	$1.5 \times 10^7 \text{ cm}^{-3}$	16 %
$k(\text{OH})$	Laser photolysis + LIF ^b (Lou et al., 2010)	180 s	0.3 s^{-1}	0.5 s^{-1}
NO	Chemiluminescence (Rohrer and Brüning, 1992)	180 s	4 pptv	5 %
NO ₂	Chemiluminescence (Rohrer and Brüning, 1992)	180 s	2 pptv	5 %
O ₃	Chemiluminescence (Ridley et al., 1992)	180 s	60 pptv	5 %
MACR	PTR-TOF-MS ^c (Lindinger et al., 1998; Jordan et al., 2009)	30 s	15 pptv	14 %
HONO	LOPAP ^d (Häseler et al., 2009)	300 s	1.3 pptv	10 %
HCHO	Hantzsch monitor (Kelly and Fortune, 1994)	120 s	20 pptv	5 %
CH ₃ CHO	PTR-TOF-MS ^c (Lindinger et al., 1998; Jordan et al., 2009)	30 s	50 pptv	15 %
PAN	GC ^e (Volz-Thomas et al., 2002)	600 s	25 pptv	10 %
MPAN	GC ^e (Volz-Thomas et al., 2002)	600 s	25 pptv	20 %
Photolysis frequencies	Spectroradiometer (Bohn et al., 2005)	60 s	10 %	10 %

^a Differential optical absorption spectroscopy.

^b Laser-induced fluorescence.

^c Proton-transfer-reaction time-of-flight mass spectrometry.

^d Long-path absorption photometer.

^e Gas chromatography.

acetaldehyde and formaldehyde are formed with a rate of approximately 200 pptv h^{-1} during these experiments. The OH reactivity is of the order of $(1-2) \text{ s}^{-1}$ in the absence of additional OH reactants, which can be partly explained by the presence of NO, NO₂, formaldehyde (HCHO), and acetaldehyde (CH₃CHO). RO₂ radicals of approximately $(1-2) \times 10^8 \text{ cm}^{-3}$ were immediately formed in the humidified

clean air when the chamber roof was opened. They were partly formed by photolytic processes. This is evident from reference experiments with CO, in which the RO₂ radical concentrations persisted even though OH was completely scavenged by excess CO, and so no RO₂ production is expected from the reaction of OH with organic compounds. Sources of trace gases and radicals can be well parameterized

from reference experiments, but except for the production of HONO they played only a minor role for the experiments after MACR had been injected.

2.2 Instrumentation

Trace gas and radical concentrations were measured using instruments listed in Table 2. A laser-induced fluorescence instrument (LIF) was used to measure OH, HO₂, and RO₂ concentrations simultaneously in three parallel measurement cells. RO₂ and HO₂ are detected via their conversion to OH involving reactions with NO. The signal of the HO₂ detection includes a small fraction of specific RO₂ species, which can be partly converted to OH on the same timescale (Fuchs et al., 2011). Instrument parameters were optimized to minimize this interference. For RO₂ where conversion to OH requires more than two reactions with NO (e.g. acyl peroxy radicals), the conversion efficiency is assumed to be low because of the short residence time between NO addition and OH detection in the instrument (Fuchs et al., 2008). The measured detection efficiency for MACR-derived RO₂ is similar to that of methyl peroxy radicals (i.e. they are converted to OH on the relevant timescales).

OH was also detected by a differential optical absorption spectrometer (DOAS) during two of the three experiments. As previously shown, measurements of both instruments (LIF and DOAS) usually agreed within their uncertainties during experiments in SAPHIR that were performed for the investigation of the oxidation of various organic compounds including MACR (Schlosser et al., 2007, 2009; Fuchs et al., 2012). This indicates that OH measurements were not affected by unknown interferences.

During the experiment on 11 August 2011, the OH measurements by DOAS were $0.5 \times 10^6 \text{ cm}^{-3}$ lower than those measured by means of LIF; such a difference was not observed in other experiments investigating MACR oxidation (Fuchs et al., 2012). For the analysis of data from 11 August 2011 in Fig. 2 and 5, we chose the DOAS data, which are regarded to be an absolute measurement reference (Schlosser et al., 2009).

The chemical lifetime of OH was measured applying a combination of (1) flash photolysis producing OH by ozone photolysis at 266 nm in a reaction cell under slow-flow conditions and (2) time-resolved detection of OH by LIF (Lou et al., 2010). The evaluation of the pseudo-first-order decays directly gives the rate coefficient of the OH loss (OH reactivity) or inverse OH lifetime. OH regeneration from subsequent chemistry can disturb measurements (Lou et al., 2010), but was not observed during these experiments, because OH was regenerated from RO₂ radicals on a much longer timescale (see below) compared to the timescale of the OH decay in the instrument.

Organic compounds were measured with a proton-transfer-reaction time-of-flight mass spectrometry instrument (PTR-TOF-MS), nitrogen oxides and ozone with

chemiluminescence instruments, and nitrous acid with a long-path absorption photometer (LOPAP). During one of the experiments, two peroxyacyl nitrates – PAN and MPAN – which serve as reservoirs for peroxy radicals and nitrogen oxides during MACR oxidation, were detected via gas chromatography (GC).

2.3 Model calculations

Time series of measurements were compared to calculations using the Master Chemical Mechanism version 3.2 (MCM) (Jenkin et al., 1997; Saunders et al., 2003), available at <http://mcm.leeds.ac.uk/MCM>. Throughout the paper “MCM” denotes the mechanism in its current version, 3.2. The MCM provides near-explicit mechanisms of the atmospheric degradation of organic compounds. In addition to the chemistry from the MCM, chamber-specific properties were included in the model calculations. Dilution of trace gases due to the replenishment of zero air was modelled from monitored rates of the dilution flow. The dependence of source strengths for HONO, HCHO, and CH₃CHO on radiation, relative humidity, and temperature were taken from parameterizations described earlier (Rohrer et al., 2005; Karl et al., 2006). The source strengths were scaled in order to match formation of NO_x, HCHO, and CH₃CHO during the zero-air part of the experiment. The part of the OH reactivity (approximately 1 s^{-1}) which could not be explained by the presence of measured OH reactants was treated as an OH reactant of constant concentration, which converts OH to HO₂ like CO does. The value of this “background” OH reactivity was determined from the measured OH reactivity at the start of the experiment (dark chamber), when only zero air and water vapour was present. Also, RO₂ radicals were formed in the sunlit chamber from unknown sources. A photolytic RO₂ source was implemented in the model, which was similarly parameterized as the empirical functions for the HONO and HCHO sources. Test experiments with only humidified zero air in the chamber showed that RO₂ time series can be well described by this procedure. Effects on measurements during VOC oxidation experiments are small.

The model was constrained by measurements of temperature, pressure, calculated dilution rates, measured water vapour mixing ratios, and photolysis frequencies for NO₂, HCHO, O₃, MACR, and HONO. Photolysis frequencies and relative humidity constrained the calculated chamber sources for HONO, HCHO, and CH₃CHO. Photolysis frequencies that were not measured were first calculated by a MCM (version 3.1) function for clear-sky conditions and then scaled by the ratio of the measured and calculated NO₂ photolysis frequencies to account for reductions of the solar radiation by clouds and the transmission of the Teflon film. Constrained parameters were re-initialized on a 1 min time grid. The injection of trace gases (O₃, MACR) was modelled as sources which were turned on for the time of the injection. The source strength for ozone was adjusted to match the

measured concentrations right after the injection, and that for MACR was adjusted to match the change in the measured OH reactivity. Otherwise, trace gas concentrations were calculated by the model.

Modelled HO₂ concentrations presented here are the sum of calculated HO₂ and a fraction of specific RO₂ that is an interference in the HO₂ measurements HO₂ measurements (named HO₂^{*} in Lu et al. (2012)), and thus measurements can be compared to calculations. Model calculations taking RO₂ conversion efficiency from characterization experiments of the instrument suggest that the contribution of this interference to the entire HO₂ detection was less than 5 % for these experiments, most of which is caused by RO₂ from MACR. Calculated RO₂ concentrations that are shown in the following only include those RO₂ species that are efficiently converted to OH in the RO₂ measurement channel of the LIF instrument.

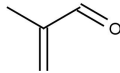
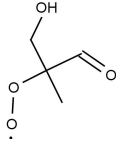
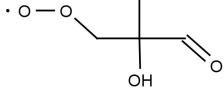
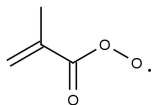
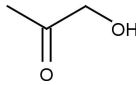
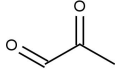
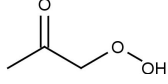
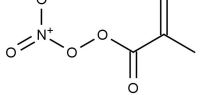
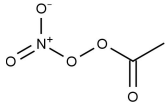
3 Results and discussion

3.1 Time series of trace gas concentrations

Once the humidified clean air is exposed to sunlight, HONO is formed on the chamber walls. Its photolysis increases the concentrations of NO_x and OH (Fig. 1). During this initial phase of the experiment, the OH reactivity is only approximately 1 s⁻¹, and so maximum OH concentrations of 1 × 10⁷ cm⁻³ are reached (OH concentrations in Fig. 1 are scaled by a factor of 0.5 during this part of the experiment). MACR injections increase the OH reactivity to up to 13.5 s⁻¹, and as a result OH concentrations drop to (1–1.5) × 10⁶ cm⁻³. The maximum MACR mixing ratio after the last injection is 14 ppbv. OH dominantly reacts with MACR during the entire experiment (e.g. 14 ppbv MACR corresponds to an OH reactivity of 10 s⁻¹). Reaction of OH with MACR initiates a reaction chain that produces RO₂ and HO₂, which includes reactions with NO, and as a result RO₂ and HO₂ concentrations increase in the presence of MACR. Similarly, concentrations of radical reservoir species peroxyacetyl nitrate and peroxy methacryloyl nitrate, PAN and MPAN (Table 3), increase after each MACR injection. These species are products of the reaction of acyl peroxy radicals with NO₂. MPAN and PAN are thermally unstable (Roberts and Bertman, 1992), and thus a thermal equilibrium is established. Because PAN is also formed from acetaldehyde in the sunlit chamber, the PAN mixing ratio starts increasing before MACR is injected. The NO concentration is nearly constant over the course of the experiment, with a mixing ratio of approximately 90 pptv.

Model calculations applying MCM give OH concentrations, which are approximately 50 % lower than measurements during the MACR oxidation part of the experiment (Fig. 1). The increasing difference between measured and modelled MACR indicates that less MACR is oxidized in the

Table 3. Chemical structure of MACR and products from its oxidation with OH. Acronyms are taken from the MCM.

MACR (methacrolein)	
MACRO2	
MACROHO2	
MACO3	
ACETOL (hydroxyacetone)	
MGLYOX (methylglyoxal)	
HYPERACET (hydroperoxyacetone)	
MPAN (peroxy methacryloyl nitrate)	
PAN (peroxyacetyl nitrate)	

model during the experiment, supporting that OH concentrations in the chamber are indeed larger than calculated. The overprediction of MACR would change the OH reactivity by only 10–15 %. This change in the modelled reactivity is not significant.

The decay of measured MACR concentrations can be used to calculate average OH concentrations following the approach described by Poppe et al. (2007). In this approach, the difference of MACR concentrations between two injections is related to the average OH concentrations taking the degradation of MACR by OH and the dilution in the chamber into account. The average OH concentrations required to explain the observed MACR decays are 4 × 10⁶, 2.5 × 10⁶, and 1.4 × 10⁶ cm⁻³ between the first and second, second and third, and after the third MACR injection, respectively. This

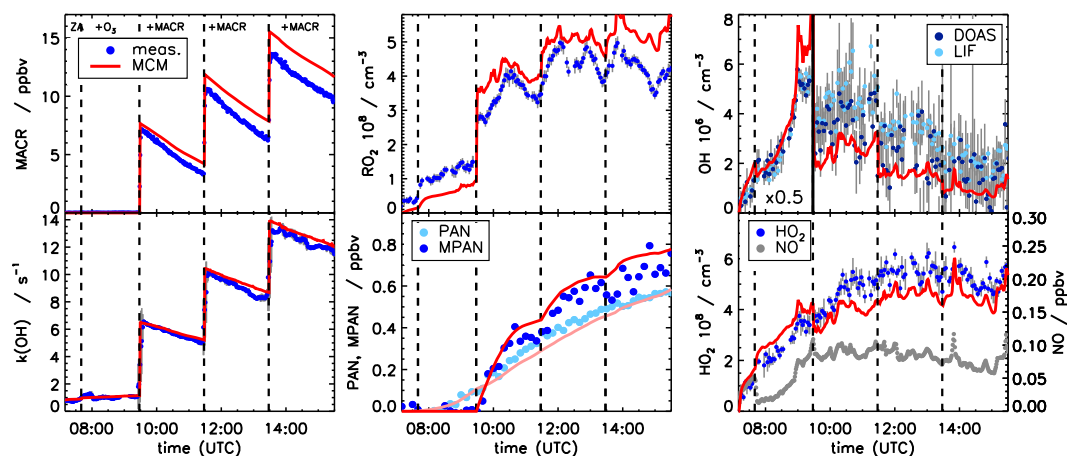


Figure 1. Measured and modelled time series of MACR, $k(\text{OH})$, PAN, MPAN, RO_2 , HO_2 , OH, and NO for the experiment on 11 August 2011. OH concentrations prior to the addition of MACR (“ZA”, “+O₃”) are scaled by a factor of 0.5. Model calculations applying MCM underestimate OH concentrations. Measured and modelled HO_2 concentrations include a small fraction of RO_2 radicals, which show up as an interference in the HO_2 detection (less than 5 % of the entire concentration). RO_2 radical concentrations shown here do not include the class of acyl peroxy radicals, which cannot be detected by the instrument.

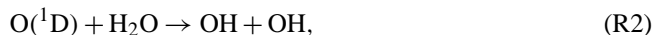
is again consistent with larger measured OH concentrations compared to the modelled OH concentrations.

The reaction of OH with MACR produces three RO_2 species (MCM names: MACRO2, MACROHO2, MACO3; Table 3). Measured RO_2 radical concentrations are reproduced by model calculations. Acyl peroxy radicals like MACO3 are detected by the LIF instrument with low sensitivity (see above). However, the good model–measurement agreement of MPAN and PAN mixing ratios, which are formed from MACO3, indicates that model calculations reproduce MACO3 concentrations. The shape of the temporal behaviour of MPAN mixing ratios is determined by the thermal equilibrium between MPAN and MACO3, forcing the fast build up of MPAN after each methacrolein injection. At later times, the concentration of MPAN declines as the production of MACO3 from MACR decreases. HO_2 concentrations are slightly underestimated, but the difference is within the uncertainty of measurements (Table 2).

In general, the description of radical species by the MCM during the part of the experiment before OH reactants are injected into the chamber is expected to be less accurate because (1) the OH reactivity is mostly caused by unknown species and (2) radical sources and sinks are not well defined. After the initial phase of the experiment, the OH reactivity is dominated by MACR. Under these conditions, a much better model–measurement agreement is expected, because chamber-specific properties like the low OH reactivity from unknown species do not play a role any longer. This can be seen in similar experiments in which CO or butene was the dominant OH reactant. A model–measurement agreement for radical species within 30 % is achieved in these reference experiments, which are performed on a regular basis in the chamber.

3.2 OH budget analysis

The underprediction of the OH concentration in the model could be caused either by an overestimation of the OH loss or by an underestimation of the OH production. The relatively good agreement of the measured OH reactivity with model calculations (Fig. 1) indicates that an OH source is missing in the model. The missing production rate can be analysed by a model-independent approach by comparing the OH production and destruction rates of known processes (Hofzumahaus et al., 2009). Primary OH sources in the chamber are O₃ and HONO photolysis. Furthermore, OH is produced from radical recycling via the reaction of HO_2 with NO:



All three contributions to the OH production can be calculated using only experimental data. Also, the OH reactivity and the OH concentration were measured so that the OH destruction rate can be calculated. Figure 2 shows time series of the OH production (summed up as coloured areas) and of the OH destruction rate for the experiment on 11 August 2011. Before MACR is injected to the chamber air, the OH production is balanced by its destruction, as expected for a short-lived species like OH under steady-state conditions. However, during the MACR oxidation part of the experiment, the calculated OH destruction rate is on average twice as high as the sum of OH production from radical recycling via the $\text{HO}_2 + \text{NO}$ reaction and O₃ and HONO photolysis. As discussed below, potential OH production from the

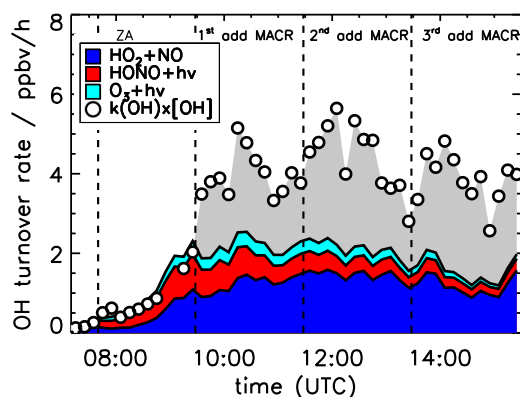


Figure 2. OH budget for the experiment on 11 August 2011. Black circles give the turnover of the OH destruction rate calculated from measured OH concentrations (DOAS) and the measured OH reactivity. Coloured areas sum up the OH production from sources that can be calculated from measurements. OH production from the reaction of acyl peroxy radicals with HO₂ is negligible here (see discussion). Because of the short lifetime of OH, the production and destruction rates are expected to be equal at all times. The grey area denotes the difference between calculated destruction and production rate. Whereas the OH budget is closed before the injection of MACR (“ZA”), on average half of the OH source is missed during MACR oxidation. HO₂ measurements and calculations include a small interference from specific RO₂ (see text for details).

reaction of HO₂ with RO₂ would be low. The grey shaded area in Fig. 2 indicates the additional OH production from an unknown source that is needed to balance the OH destruction (“missing OH source”). Apparently, the missing OH source is linked with the degradation of MACR by OH.

In the following, the data from all experiments are collectively analysed to determine the missing OH source. This is justified because conditions of the experiments were similar (Table 1). The time-resolved missing OH source shows considerable variability over the course of all experiments, but no significant trend with time is seen in the data (Fig. 3, upper panel). This indicates that the additional OH is most likely not produced from longer-lived first-generation organic products of the MACR oxidation such as hydroxyacetone. These products would accumulate over the course of the experiment because they are less reactive towards OH (Butkovskaya et al., 2006). Therefore, increasing OH production would be expected if an additional OH were produced from these species.

Part of the variability of the time series of the missing OH production rate is caused by the variability of the production rate of RO₂ formed in the reaction of MACR with OH (Fig. 3). Here, the RO₂ production rate is calculated from measured OH and MACR concentrations assuming that every reaction of OH with MACR yields one RO₂ radical. Plotting the missing OH production rate against the RO₂ formation rate (Fig. 3) reveals a clear correlation between both values. This suggests that OH is formed from an RO₂ reaction

channel missing in the MCM mechanism. The slope of the correlation would be the amount of OH that is additionally produced from each RO₂ radical. A weighted linear fit with a fixed zero offset gives a value of 0.77 ± 0.31 . Here, the 1σ uncertainty of ± 0.31 is determined by the 1σ accuracy of measurements that are included in both coordinates of the correlation (Fig. 3), giving an uncertainty of the slope of approximately $\pm 40\%$.

This additional reaction channel competes with the reaction of RO₂ with NO, which finally also regenerates OH, and the reaction of RO₂ with HO₂, which is a radical termination reaction forming peroxides (ROOH):



Reaction (R7) could be either a unimolecular reaction or could involve a reaction partner whose concentration is highly correlated with the RO₂ production. The calculated yield of 0.77 ± 0.31 OH from each RO₂ radical needed to close the OH budget can be regarded as the fractional contribution of Reaction (R7) to the RO₂ loss. The large value indicates that this reaction channel is an important pathway for conditions of these experiments (NO mixing ratios less than 100 pptv and HO₂ concentrations less than $6 \times 10^8 \text{ cm}^{-3}$).

3.3 Modifications of the MACR oxidation scheme

3.3.1 Generic OH recycling with X

A large discrepancy between measured and modelled OH concentrations has been observed in several field campaigns. In order to explain the high OH concentrations in some field campaigns, a generic recycling of OH radicals by a constant amount of an unknown compound, X, was assumed that would convert peroxy radicals to OH like NO does, but without accompanying ozone production (Hofzumahaus et al., 2009; Lu et al., 2012, 2013):



Different amounts of X (in units of NO equivalents) were required: Pearl River delta, 800 pptv (Hofzumahaus et al., 2009; Lu et al., 2012); Beijing, 400 pptv (Lu et al., 2013); and Borneo, 700 pptv (Whalley et al., 2011). The nature of X, however, remained unclear, and thus this mechanism could only serve as an empirical description. Recently, generic OH recycling was also applied in order to describe fast OH regeneration from isoprene oxidation by OH in experiments in the SAPHIR chamber (Fuchs et al., 2013). A constant NO equivalent of 100 pptv was required in this case. It was shown that the effect of a generic OH recycling by X had the same effect as OH production from RO₂ radical isomerization and decomposition reactions.

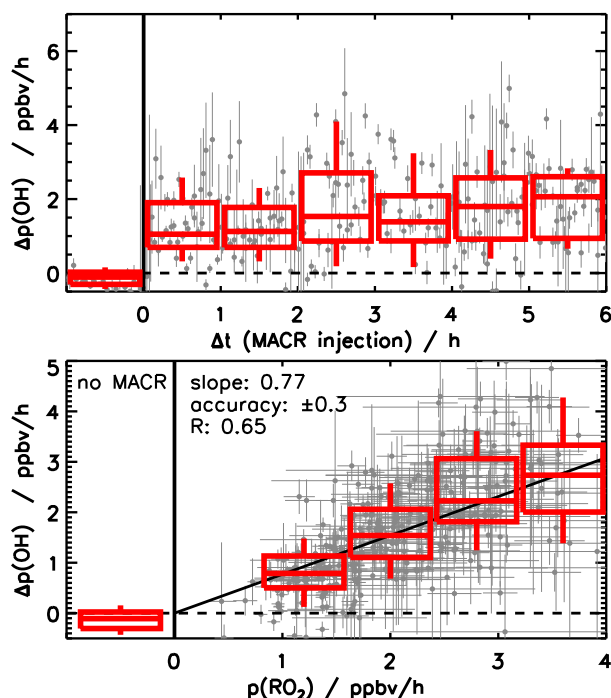


Figure 3. Scatter plot of the missing OH source ($\Delta p(\text{OH})$) and (1) the time that has elapsed since the first MACR injection (upper panel) and (2) production of RO_2 from the reaction of MACR and OH (lower panel). Grey dots give individual data points with statistical errors for all three experiments (Table 1); boxes show 25 and 75 % percentiles and whiskers 10 and 90 % percentiles. The value of the linear correlation coefficient of $R = 0.65$ shows the good correlation between the RO_2 production from MACR and the missing OH source. The slope of a weighted linear fit (black line) suggests that on average 0.77 OH radicals are recycled from RO_2 for conditions of these experiments. The error of 0.3 is calculated from the accuracy of measurements.

Generic OH recycling by X is also tested for MACR oxidation experiments here in order to see whether this empirical mechanism can also describe observations like shown for isoprene oxidation experiments. In fact, all observations including those of OH and MACR can be reproduced if the mixing ratio of X is assumed to be equivalent to 50 pptv NO (Figs. 4 and 5). This amount of X is only half of what was found for isoprene oxidation for similar conditions (Fuchs et al., 2013), and is approximately 10 times lower compared to the amount of X that was needed to explain the above-mentioned field observations.

3.3.2 RO_2 isomerization reactions

The reaction of OH with MACR either leads to OH addition to the C=C double bond or H abstraction from the CHO group (Tuazon and Atkinson, 1990; Orlando et al., 1999). OH adds dominantly to the external olefinic carbon atom (yield MCM: 47 %; Fig. 6), forming an RO_2 radical after

reaction with O_2 (MCM: MACRO2). OH addition to the internal carbon atom is less likely (yield MCM: 8 %) and forms a different RO_2 radical after reaction with O_2 (MCM: MACROHO2). H abstraction from the CHO group of MACR leads to the formation of an acyl peroxy radical after reaction with O_2 (MCM: MACO3, yield 45 %; Fig. 6).

Recent work has shown that the yield of OH from the reaction of HO_2 with acyl peroxy radicals like MACO3 could be larger than previously thought (Dillon and Crowley, 2008; Taraborrelli et al., 2012). The chemical model used in this work, MCM, assumes an OH yield of 0.44 for the reaction of HO_2 with MACO3, whereas a yield of <0.7 was found for the simplest acyl peroxy radical CH_3CO_3 (Dillon and Crowley, 2008; Groß, 2014). Although the qualitative behaviour of the missing OH source would be consistent with a larger OH yield from the reaction of HO_2 with MACO3 or other acyl peroxy radicals (Fig. 3), the turnover rates of these reactions are too low to significantly increase the OH production rate. Doubling of the OH yield from the reaction of MACO3 with HO_2 would increase the OH production rate by less than 0.1 ppbv h^{-1} and from the reaction of CH_3CO_3 with HO_2 less than 0.05 ppbv h^{-1} , much lower than the missing OH production rate.

Quantum chemical calculations showed that RO_2 isomerization with subsequent decomposition could lead to fast OH regeneration from RO_2 from isoprene via 1,5-H-shift or 1,6-H-shift isomerization with subsequent decomposition of the products (Peeters et al., 2009; Peeters and Müller, 2010; da Silva et al., 2010). Similar reaction schemes have also been proposed for MACR (Peeters et al., 2009; Crouse et al., 2012; Asatryan et al., 2010; da Silva, 2012). A 1,5-H shift for MACRO2 with subsequent decomposition would produce methylglyoxal, formaldehyde, and OH. A rate constant of less than 0.008 s^{-1} at 303 K has been calculated (Peeters et al., 2009; Crouse et al., 2012). Because additional OH from this isomerization reaction applies only for one RO_2 isomer (MACRO2) from the OH + MACR reaction and the rate constant is relatively low, the calculated amount of additional OH produced from this isomerization channel is rather low. Time series of modelled radical and trace gas concentrations are shown in Fig. 4 for this case, and Fig. 5 displays the ratio of measured to modelled OH concentrations. The 1,5-H shift only slightly improves the model–measurement agreement.

In addition to the 1,5-H shift of MACRO2, a much faster 1,4-H shift for MACRO2 and a fast 1,5-H shift for MACROHO2 with an isomerization rate constant of $(0.5 \pm 0.3) \text{ s}^{-1}$ at 296 K for both reactions have been suggested (Crouse et al., 2012). The 1,5-H shift of the aldehyde H atom in MACROHO2 would produce hydroperoxyacetone (MCM: HYPERACET; Table 3), CO, and HO_2 . The 1,4-H shift of MACRO2 would lead to the formation of hydroxyacetone, CO, and OH (Crouse et al., 2012) (Fig. 6). A laboratory study (Crouse et al., 2012) has shown that hydroxyacetone concentrations which were measured in MACR

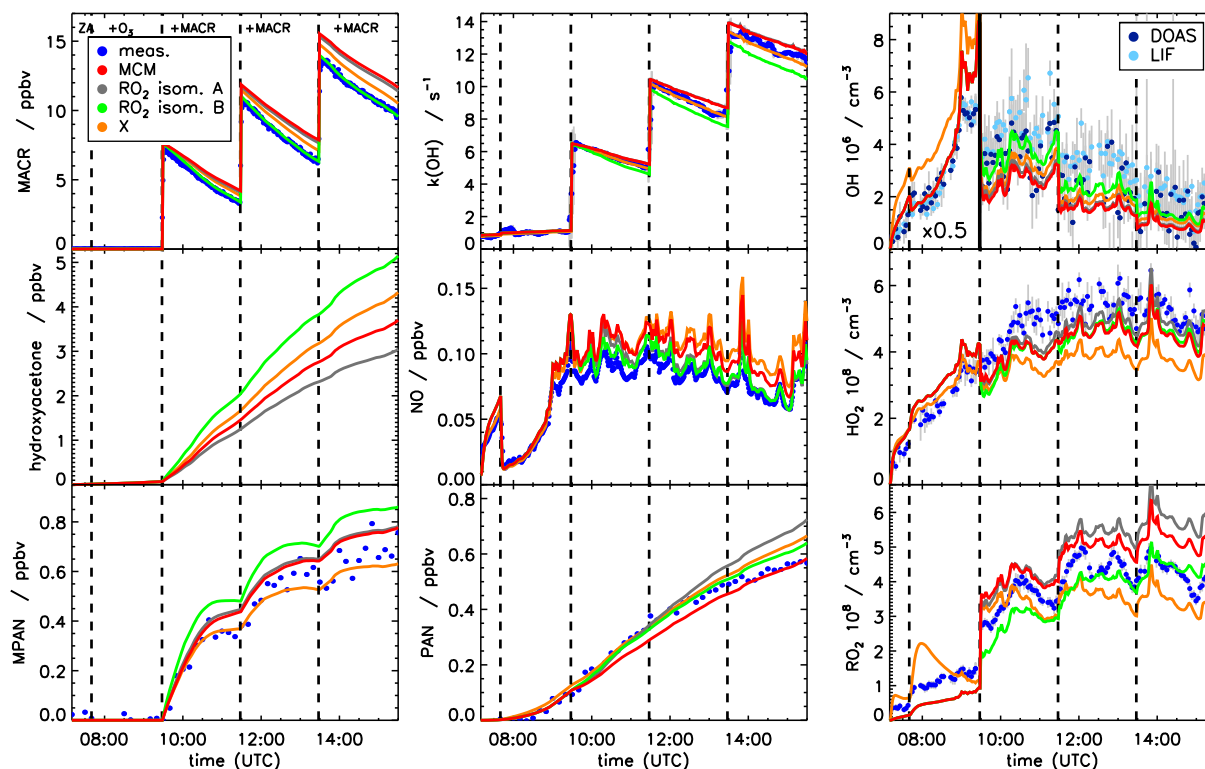


Figure 4. Measured and modelled time series of MACR, $k(\text{OH})$, PAN, MPAN, RO_2 , HO_2 , OH, and NO for the experiment on 11 August 2011. OH prior to the addition of MACR is scaled by a factor of 0.5. Different model runs were performed applying the MCM, the MCM with two additional RO_2 isomerization reaction schemes (case A and B; see Table 4), and MCM with additional generic OH recycling (“X”) with an NO equivalent of 50 pptv. Only calculated hydroxyacetone concentrations are shown, because hydroxyacetone was not measured during experiments.

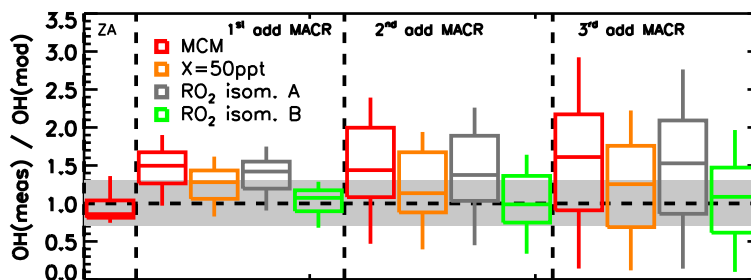


Figure 5. Ratio of measured (DOAS) to modelled OH concentrations for the four parts of the experiment on 11 August 2011 applying different model approaches: MCM, MCM with additional generic OH recycling (“X”), and MCM with additional RO_2 isomerization schemes (case A and B; see Table 4). The grey shaded area gives the range of agreement of modelled and calculated OH concentrations that is achieved in reference experiments.

oxidation experiments with low NO concentrations are much larger than expected. According to the study by Crouse et al. (2012), this result is consistent with the fast production of hydroxyacetone in the 1,4-H-shift isomerization channel of MACRO2. Application of a temperature dependence as suggested in the literature (Crouse et al., 2012) yields a rate constant of 0.66 s^{-1} at the temperature during the experiment on 11 August 2011 (301 K). For conditions of this experiment, more than 95 % of the MACRO2 would undergo

the 1,4-H shift. Also, the branching ratio of the 1,5-H shift for MACROHO2 would be 95 % if the reaction rate constant were similarly high as suggested. Figure 4 shows time series of concentrations and Fig. 5 the ratio of measured to modelled OH concentrations (case B) if both the 1,4-H shift of MACRO2 and the 1,5-H shift of MACROHO2 are included. All observations, especially OH concentrations, are matched in this case. Most of the additional OH is formed by the 1,4-H-shift reaction of MACRO2. At the end of the experiment,

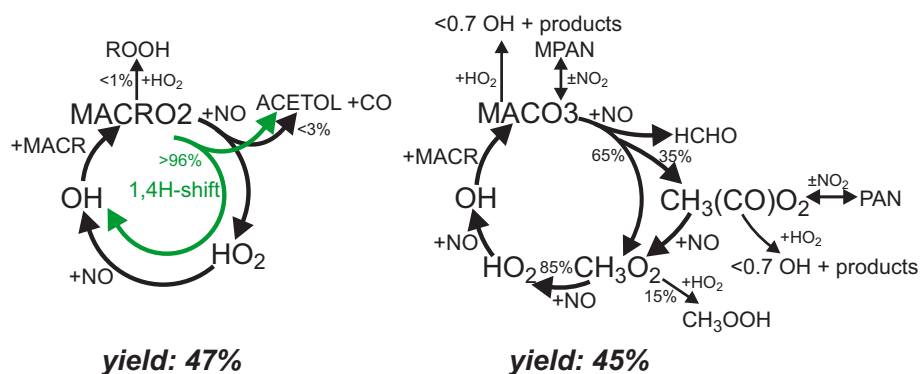


Figure 6. Schematics of radical recycling from the reaction of MACR with OH taken from MCM (black arrows) showing the reactions which were of importance for conditions of these experiments. H-atom abstraction of the CHO group in MACR leads to the formation of an acyl peroxy radical (MACO3: yield 45 %), whereas OH addition to the C=C double bond forms two hydroxyalkoxy radical isomers (RO₂: MACRO2, yield 47 %, and MACROHO2, yield 8 % (not shown here)). Green arrows indicate the 1,4-H-shift reaction of MACRO2 (Crouse et al., 2012) (the less important 1,5-H shift is not shown here). Branching ratios are given for conditions of the experiment on 11 August 2011 (NO = 90 pptv, HO₂ = 5 × 10⁸ cm⁻³, T = 301 K) if the fast unimolecular reaction is included.

the isomerization mechanism is expected to increase the hydroxyacetone mixing ratio by 1.5 ppbv compared to MCM calculations (Fig. 4).

For conditions of these experiments, the ozone production rate is only a little less (< 10 %) when the model modification including the RO₂ isomerization reactions is applied compared to the base-case MCM model run. This can be seen in the small changes in the NO mixing ratio and peroxy radical concentrations. The missing contribution of MACRO2 to the ozone production when isomerization of MACRO2 is the dominant pathway is partly balanced by the faster production of other RO₂ radicals such as CH₃O₂ which contribute to the ozone production due to the enhanced OH level. For the same reason, the ratio of NO₂-to-NO mixing ratios also does not change much (< 15 %) between the two models.

Model calculations with variation of the 1,4-H-shift isomerization rate constant were performed to estimate the sensitivity of calculated OH concentrations for experiments here. Decreasing the isomerization rate to a value, for which the median of the difference between measured and modelled OH has a maximum value of 30 % (the agreement that is expected from reference experiments), gives a lower limit of the rate constant constant of 0.03 s⁻¹. In this case, the MACRO2 isomerization reaction would regenerate 50 % of the OH radicals that were consumed in the MACR+OH reaction to produce MACRO2. This result is independent of the choice of OH data from either the DOAS or the LIF instrument, because the lower limit is determined by the slightly lower OH concentrations measured by means of DOAS compared to LIF (see above). In contrast, modelled OH concentrations are insensitive to a reaction rate constant larger than suggested in the literature (Crouse et al., 2012). In this case, MACRO2 and also MACROHO2 radicals nearly exclusively undergo isomerization for conditions of this experiment (Fig. 6). The yield of OH regenerated by isomerization becomes limited

by the yields of MACRO2 and MACROHO2 from the reaction of MACR with OH. This implies that the isomerization reaction is much faster than all other reaction of MACRO2 and MACROHO2 for conditions of the experiment. Our OH yield of 0.77 for each OH radical consumed by MACR (Fig. 3) is larger than the yield of 0.55 predicted by the model calculation if MACRO2 and MACROHO2 is completely converted to OH in the isomerization reaction. This is, however, not a contradiction considering the relative large uncertainty of ±0.3 (1σ) of our experimental value and the uncertainty of the model. Thus, our SAPHIR experiments presented in this work do not allow an upper limit of the 1,4-H-shift isomerization rate constant to be determined.

In addition to thermal decomposition of RO₂, another reaction scheme has been proposed from quantum-chemical calculations (da Silva, 2012; Asatryan et al., 2010). This suggests that the vibrationally excited adduct of MACR and OH reacts with O₂ on a similar timescale as collisional deactivation of the adduct takes place. As a consequence, approximately 20 % of the MACR–OH adduct would react with O₂ and form “double-activated” RO₂ radicals, which can then decompose (da Silva, 2012). Decomposition of the double-activated RO₂ would lead to the formation of either methylglyoxal, formaldehyde, and OH or hydroxyacetone, CO, and OH. In the result, this mechanism is equivalent to the 1,4- and 1,5-H-shift isomerization reactions (Table 4) and would be equivalent to a maximum isomerization rate constant of 0.007 s⁻¹ in order to yield a branching ratio of maximum 20 % for conditions of these experiments. As shown above, more than 50 % of MACRO2 needs to immediately regenerate OH in order to explain our observations, much larger than the 20 % yield of double-activated RO₂. Therefore, this mechanism alone is not sufficient to bring calculations and measurements into agreement. Nevertheless, part of the discrepancy could be potentially due to the decomposition of

Table 4. Modification of MCM oxidation scheme for MACR. The “X” mechanism adds generic recycling of OH via reaction of peroxy radicals with a compound, X, which behaves like NO. The two cases of RO₂ isomerization produces additional OH via RO₂ isomerization with subsequent decomposition of the products.

	Reaction	Rate constant	Reference
X	RO ₂ + X → HO ₂	$2.7 \times 10^{-12} \exp(360\text{K}/T) \text{ s}^{-1} \text{ cm}^3$	Hofzumahaus et al. (2009)
	HO ₂ + X → OH	$3.45 \times 10^{-12} \exp(270\text{K}/T) \text{ s}^{-1} \text{ cm}^3$	
RO ₂ isom. A	MACRO2 $\xrightarrow{1,5\text{-H shift}}$ MGLYOX + OH + HCHO	0.008 s ⁻¹	Peeters et al. (2009)
RO ₂ isom. B	MACRO2 $\xrightarrow{1,4\text{-H shift}}$ ACETOL + OH + CO	$2.9 \times 10^7 \exp(-5300\text{K}/T) \text{ s}^{-1}$	Crouse et al. (2012)
	MACRO2 $\xrightarrow{1,5\text{-H shift}}$ MGLYOX + OH + HCHO	0.0018 s ⁻¹	
	MACROHO2 $\xrightarrow{1,5\text{-H shift}}$ HYPERACET + CO + HO ₂	0.5 s ⁻¹	

“double-activated” RO₂, because it is not possible to distinguish between both mechanisms in our experiments.

The 1,4-H-shift isomerization rate constant that is required to explain observations from MACRO2 isomerization ($> 0.03 \text{ s}^{-1}$) is equivalent to the reaction of MACRO2 with more than 150 pptv NO. This value is larger than the amount of X that is needed to describe measured OH concentrations in the “X” mechanism (see above). In the X mechanism 50 pptv X is equivalent to an additional RO₂ loss rate of 0.01 s^{-1} . However, in the X mechanism, additional OH is recycled by all RO₂ species, with the result that the overall impact is larger than that from MACRO2 alone. Therefore, the 1,4-H-shift isomerization rate constant cannot be directly compared to the loss rate of MACRO2 with X in the X mechanism.

4 Summary and conclusions

Measured OH concentrations during MACR oxidation experiments in the atmosphere simulation chamber SAPHIR are underestimated by the MCM by approximately 50 % (NO mixing ratios approximately 90 pptv; HO₂ concentrations approximately $5 \times 10^8 \text{ cm}^{-3}$ and $T = 301 \text{ K}$). The analysis of the OH budget reveals that an additional OH source is required to balance the measured OH destruction rate. Experiments allow for the overall strength of the OH source to be constrained regardless of the exact chemical mechanism that is responsible for the OH production.

Production of OH from unimolecular isomerization and decomposition reactions of RO₂ radicals (Peeters et al., 2009; Crouse et al., 2012; Asatryan et al., 2010; da Silva, 2012) and the decomposition of double-activated RO₂ (Asatryan et al., 2010; da Silva, 2012) give the same products. These mechanisms produce OH from RO₂ without reactions with NO, consistent with observations here. However, only the 1,4-H shift (Crouse et al., 2012) is fast enough to bring observations and calculations into agreement, whereas the 1,5-H shift and decomposition of double-activated RO₂ only slightly improves the agreement between model calculations

and measurements. Model calculations are consistent with the observations within the expected agreement if the reaction rate constant for the 1,4-H shift of the RO₂ isomer MACRO2 is faster than 0.03 s^{-1} . In this case, at least 50 % of MACRO2 undergoes the 1,4-H-shift reaction instead of reacting with NO or HO₂ as assumed in the MCM. Thus, the 1,4-H-shift reaction is a competitor to the reaction of MACRO2 with 150 pptv NO or even higher NO mixing ratios using the rate constant by Crouse et al. (2012).

A yield of 0.77 ± 0.31 for additionally produced OH is found from the OH budget analysis in these experiments. For unimolecular RO₂ reactions of MACRO2 and MACROHO2 as suggested by Crouse et al. (2012), 0.55 additional OH can be explained. This value is comparable to the overall yield of OH from unimolecular RO₂ reactions produced from isoprene-derived RO₂ (38–45 %) for similar conditions as inferred by Fuchs et al. (2013). However, the impact of these reaction pathways is less for MACR compared to isoprene for two reasons: (1) typical MACR mixing ratios are smaller compared to isoprene, because MACR is a product of isoprene degradation with a yield of less than 30 % (Galloway et al., 2011); (2) its reaction rate constant with OH is 3.5 times lower, and so the MACR oxidation rate and therefore the production rate of MACR derived RO₂ is lower; and (3) the total OH production from RO₂ isomerization reactions is limited by the yield of MACRO2 and MACROHO2.

During field campaigns in the Amazon rainforest when unexpectedly large OH was found, isoprene was the dominant OH reactant. Measurements of the sum of methyl-vinyl ketone (MVK) and MACR also indicate substantial amounts of MACR (Kubistin et al., 2010). Assuming that at most half of the measured MVK + MACR concentration was MACR, MACR mixing ratios were only 20 % of the mixing ratio of isoprene when the largest discrepancy between measured and predicted OH was found (Kubistin et al., 2010). Given the smaller reaction rate constant of MACR with OH, the contribution of additional OH from MACR oxidation was significant, but most likely much smaller compared to that from isoprene. Because additional OH production from isoprene alone can only explain a smaller part of the entire gap

between measured and predicted OH (Fuchs et al., 2013), the contribution of additional OH from MACR derived RO₂ is most likely not large enough to close the remaining gap. During field measurements in China, MACR oxidation played only a minor role (Lou et al., 2010); therefore the impact of additional OH recycling from MACR-derived RO₂ is rather small. Nevertheless, results here show that the class of RO₂ isomerization reactions plays an important role at atmospheric conditions with low NO concentrations.

Acknowledgements. This work was supported by the EU FP-7 programme EUROCHAMP-2 (grant agreement no. 228335) and by the EU FP-7 programme PEGASOS (grant agreement no. 265307). S. Nehr and B. Bohn thank the Deutsche Forschungsgemeinschaft for funding (grant BO 1580/3-1). The authors thank A. Buchholz, P. Schlag, F. Rubach, H.-C. Wu, S. Dixneuf, M. Vietz, P. M \ddot{u} sgen, and M. Bachner for additional measurements during this campaign and technical support. The authors also thank G. da Silva for helpful discussions.

The service charges for this open access publication have been covered by a Research Centre of the Helmholtz Association.

Edited by: P. O. Wennberg

References

- Asatryan, R., da Silva, G., and Bozelli, J. W.: Quantum chemical study of the acrolein (CH₂CHCHO) + OH + O₂ reactions, *J. Phys. Chem. A*, 114, 8302–8311, doi:10.1021/jp104828a, 2010.
- Bohn, B., Rohrer, F., Brauers, T., and Wahner, A.: Actinometric measurements of NO₂ photolysis frequencies in the atmosphere simulation chamber SAPHIR, *Atmos. Chem. Phys.*, 5, 493–503, doi:10.5194/acp-5-493-2005, 2005.
- Butkovskaya, N. I., Pouvesle, N., Kukui, A., Mu, Y., and Le Bras, G.: Mechanism of the OH-initiated oxidation of hydroxyacetone over the temperature range 236–298 K, *J. Phys. Chem. A*, 110, 6833–6843, doi:10.1021/jp056345r, 2006.
- Carslaw, N., Creasey, D. J., Harrison, D., Heard, D. E., Hunter, M. C., Jacobs, P. J., Jenkin, M. E., Lee, J. D., Lewis, A. C., Pilling, M. J., Saunders, S. M., and Seakins, P. W.: OH and HO₂ radical chemistry in a forested region of north-western Greece, *Atmos. Environ.*, 35, 4725–4737, doi:10.1016/s1352-2310(01)00089-9, 2001.
- Crouse, J. D., Paulot, F., Kjaergaard, H. G., and Wennberg, P. O.: Peroxy radical isomerization in the oxidation of isoprene, *Phys. Chem. Chem. Phys.*, 13, 13607–13613, doi:10.1039/C1CP21330J, 2011.
- Crouse, J. D., Knap, H. C., Ornsø, K. B., Jørgensen, S., Paulot, F., Kjaergaard, H. G., and Wennberg, P. O.: On the atmospheric fate of methacrolein: 1. Peroxy radical isomerization following addition of OH and O₂, *J. Phys. Chem. A*, 116, 5756–5762, doi:10.1021/jp211560u, 2012.
- da Silva, G.: Reaction of methacrolein with the hydroxyl radical in air: incorporation of secondary O₂ addition into the MACR + OH master equation, *J. Phys. Chem. A*, 116, 5317–5324, doi:10.1021/jp303806w, 2012.
- da Silva, G., Graham, C., and Wang, Z.-F.: Unimolecular β -hydroxyperoxy radical decomposition with OH recycling in the photochemical oxidation of isoprene, *Environ. Sci. Technol.*, 44, 250–256, doi:10.1021/es900924d, 2010.
- Dillon, T. J. and Crowley, J. N.: Direct detection of OH formation in the reactions of HO₂ with CH₃C(O)O₂ and other substituted peroxy radicals, *Atmos. Chem. Phys.*, 8, 4877–4889, doi:10.5194/acp-8-4877-2008, 2008.
- Dorn, H.-P., Brandenburger, U., Brauers, T., and Hausmann, M.: A new in-situ laser long-path absorption instrument for the measurement of tropospheric OH radicals, *J. Atmos. Sci.*, 52, 3373–3380, 1995.
- Fuchs, H., Hofzumahaus, A., and Holland, F.: Measurement of tropospheric RO₂ and HO₂ radicals by a laser-induced fluorescence instrument, *Rev. Sci. Instrum.*, 79, 084104, doi:10.1063/1.2968712, 2008.
- Fuchs, H., Bohn, B., Hofzumahaus, A., Holland, F., Lu, K. D., Nehr, S., Rohrer, F., and Wahner, A.: Detection of HO₂ by laser-induced fluorescence: calibration and interferences from RO₂ radicals, *Atmos. Meas. Tech.*, 4, 1209–1225, doi:10.5194/amt-4-1209-2011, 2011.
- Fuchs, H., Dorn, H.-P., Bachner, M., Bohn, B., Brauers, T., Gomm, S., Hofzumahaus, A., Holland, F., Nehr, S., Rohrer, F., Tillmann, R., and Wahner, A.: Comparison of OH concentration measurements by DOAS and LIF during SAPHIR chamber experiments at high OH reactivity and low NO concentration, *Atmos. Meas. Tech.*, 5, 1611–1626, doi:10.5194/amt-5-1611-2012, 2012.
- Fuchs, H., Hofzumahaus, A., Rohrer, F., Bohn, B., Brauers, T., Dorn, H.-P., Häseler, R., Holland, F., Kaminski, M., Li, X., Lu, K., Nehr, S., Tillmann, R., Wegener, R., and Wahner, A.: Experimental evidence for efficient hydroxyl radical regeneration in isoprene oxidation, *Nat. Geosci.*, 6, 1023–1026, doi:10.1038/NNGEO1964, 2013.
- Galloway, M. M., Huisman, A. J., Yee, L. D., Chan, A. W. H., Loza, C. L., Seinfeld, J. H., and Keutsch, F. N.: Yields of oxidized volatile organic compounds during the OH radical initiated oxidation of isoprene, methyl vinyl ketone, and methacrolein under high-NO_x conditions, *Atmos. Chem. Phys.*, 11, 10779–10790, doi:10.5194/acp-11-10779-2011, 2011.
- Groß, C. B. M., Dillon, T. J., Schuster, G., Lelieveld, J., and Crowley, J. N.: Direct kinetic study of OH and O₃ formation in the reaction of CH₃C(O)O₂ with HO₂, *J. Phys. Chem. A*, 118, 974–985, doi:10.1021/jp412380z, 2014.
- Guenther, A. B., Jiang, X., Heald, C. L., Sakulyanontvittaya, T., Duhl, T., Emmons, L. K., and Wang, X.: The Model of Emissions of Gases and Aerosols from Nature version 2.1 (MEGAN2.1): an extended and updated framework for modeling biogenic emissions, *Geosci. Model Dev.*, 5, 1471–1492, doi:10.5194/gmd-5-1471-2012, 2012.
- Häseler, R., Brauers, T., Holland, F., and Wahner, A.: Development and application of a new mobile LOPAP instrument for the measurement of HONO altitude profiles in the planetary boundary layer, *Atmos. Meas. Tech. Discuss.*, 2, 2027–2054, doi:10.5194/amt-d-2-2027-2009, 2009.
- Hausmann, M., Brandenburger, U., Brauers, T., and Dorn, H.-P.: Detection of tropospheric OH radicals by long-path differential-

- optical-absorption spectroscopy: Experimental setup, accuracy, and precision, *J. Geophys. Res.*, 102, 16011–16022, doi:10.1029/97jd00931, 1997.
- Hofzumahaus, A., Rohrer, F., Lu, K., Bohn, B., Brauers, T., Chang, C.-C., Fuchs, H., Holland, F., Kita, K., Kondo, Y., Li, X., Lou, S., Shao, M., Zeng, L., Wahner, A., and Zhang, Y.: Amplified trace gas removal in the troposphere, *Science*, 324, 1702–1704, doi:10.1126/science.1164566, 2009.
- Jenkin, M. E., Saunders, S. M., and Pilling, M. J.: The tropospheric degradation of volatile organic compounds: a protocol for mechanism development, *Atmos. Environ.*, 31, 81–104, 1997.
- Jordan, A., Haidacher, S., Hanel, G., Hartungen, E., Märk, L., Seehauser, H., Schottkowsky, R., Sulzer, P., and Märk, T. D.: A high resolution and high sensitivity proton-transfer-reaction time-of-flight mass spectrometer (PTR-TOF-MS), *Int. J. Mass Spectrom.*, 286, 122–128, doi:10.1016/j.ijms.2009.07.005, 2009.
- Karl, M., Dorn, H. P., Holland, F., Koppmann, R., Poppe, D., Rupp, L., Schaub, A., and Wahner, A.: Product study of the reaction of OH radicals with isoprene in the atmosphere simulation chamber SAPHIR, *J. Atmos. Chem.*, 55, 167–187, doi:10.1007/s10874-006-9034-x, 2006.
- Kelly, T. J. and Fortune, C. R.: Continuous monitoring of gaseous formaldehyde using an improved fluorescence approach, *Int. J. Anal. Chem.*, 54, 249–263, 1994.
- Kubistin, D., Harder, H., Martinez, M., Rudolf, M., Sander, R., Bozem, H., Eerdeken, G., Fischer, H., Gurk, C., Klüpfel, T., Königstedt, R., Parchatka, U., Schiller, C. L., Stickler, A., Taraborrelli, D., Williams, J., and Lelieveld, J.: Hydroxyl radicals in the tropical troposphere over the Suriname rainforest: comparison of measurements with the box model MECCA, *Atmos. Chem. Phys.*, 10, 9705–9728, doi:10.5194/acp-10-9705-2010, 2010.
- Kuhn, U., Andreae, M. O., Ammann, C., Araújo, A. C., Brancaleoni, E., Ciccioli, P., Dindorf, T., Frattoni, M., Gatti, L. V., Ganzeveld, L., Kruijt, B., Lelieveld, J., Lloyd, J., Meixner, F. X., Nobre, A. D., Pöschl, U., Spirig, C., Stefani, P., Thielmann, A., Valentini, R., and Kesselmeier, J.: Isoprene and monoterpene fluxes from Central Amazonian rainforest inferred from tower-based and airborne measurements, and implications on the atmospheric chemistry and the local carbon budget, *Atmos. Chem. Phys.*, 7, 2855–2879, doi:10.5194/acp-7-2855-2007, 2007.
- Lelieveld, J., Butler, T. M., Crowley, J. N., Dillon, T. J., Fischer, H., Ganzeveld, L., Harder, H., Lawrence, M. G., Martinez, M., Taraborrelli, D., and Williams, J.: Atmospheric oxidation capacity sustained by a tropical forest, *Nature*, 452, 737–740, doi:10.1038/nature06870, 2008.
- Lindinger, W., Hansel, A., and Jordan, A.: On-line monitoring of volatile organic compounds at pptv levels by means of proton-transfer-reaction mass spectrometry (PTR-MS) – Medical applications, food control and environmental research, *Int. J. Mass Spectrom.*, 173, 191–241, doi:10.1016/s0168-1176(97)00281-4, 1998.
- Liu, Y. J., Herdinger-Blatt, I., McKinney, K. A. and Martin, S. T.: Production of methyl vinyl ketone and methacrolein via the hydroperoxyl pathway of isoprene oxidation, *Atmos. Chem. Phys.*, 13, 5715–5730, doi:10.5194/acp-13-5715-2013, 2013.
- Lou, S., Holland, F., Rohrer, F., Lu, K., Bohn, B., Brauers, T., Chang, C.C., Fuchs, H., Häseler, R., Kita, K., Kondo, Y., Li, X., Shao, M., Zeng, L., Wahner, A., Zhang, Y., Wang, W., and Hofzumahaus, A.: Atmospheric OH reactivities in the Pearl River Delta – China in summer 2006: measurement and model results, *Atmos. Chem. Phys.*, 10, 11243–11260, doi:10.5194/acp-10-11243-2010, 2010.
- Lu, K. D., Rohrer, F., Holland, F., Fuchs, H., Bohn, B., Brauers, T., Chang, C. C., Häseler, R., Hu, M., Kita, K., Kondo, Y., Li, X., Lou, S. R., Nehr, S., Shao, M., Zeng, L. M., Wahner, A., Zhang, Y. H., and Hofzumahaus, A.: Observation and modelling of OH and HO₂ concentrations in the Pearl River Delta 2006: a missing OH source in a VOC rich atmosphere, *Atmos. Chem. Phys.*, 12, 1541–1569, doi:10.5194/acp-12-1541-2012, 2012.
- Lu, K. D., Hofzumahaus, A., Holland, F., Bohn, B., Brauers, T., Fuchs, H., Hu, M., Häseler, R., Kita, K., Kondo, Y., Li, X., Lou, S. R., Oebel, A., Shao, M., Zeng, L. M., Wahner, A., Zhu, T., Zhang, Y. H., and Rohrer, F.: Missing OH source in a suburban environment near Beijing: observed and modelled OH and HO₂ concentrations in summer 2006, *Atmos. Chem. Phys.*, 13, 1057–1080, doi:10.5194/acp-13-1057-2013, 2013.
- Orlando, J. J., Tyndall, G. S., Fracheboud, J.-M., Estupiñan, E. G., Haberkorn, S., and Zimmer, A.: The rate and mechanism of the gas-phase oxidation of hydroxyacetone, *Atmos. Environ.*, 33, 1621–1629, doi:10.1016/s1352-2310(98)00386-0, 1999.
- Peeters, J. and Müller, J.-F.: HO_x radical regeneration in isoprene oxidation via peroxy radical isomerisations, 2: experimental evidence and global impact, *Phys. Chem. Chem. Phys.*, 12, 14227–14235, doi:10.1039/C0CP00811G, 2010.
- Peeters, J., Nguyen, T. L., and Vereecken, L.: HO_x radical regeneration in the oxidation of isoprene, *Phys. Chem. Chem. Phys.*, 11, 5935–5939, doi:10.1039/b908511d, 2009.
- Poppe, D., Brauers, T., Dorn, H.-P., Karl, M., Mentel, T., Schlosser, E., Tillmann, R., Wegener, R., and Wahner, A.: OH-initiated degradation of several hydrocarbons in the atmosphere simulation chamber SAPHIR, *J. Atmos. Chem.*, 57, 203–204, doi:10.1007/s10874-007-9065-y, 2007.
- Ren, X., Olson, J. R., Crawford, J. H., Brune, W. H., Mao, J., Long, R. B., Chen, Z., Chen, G., Avery, M. A., Sachse, G. W., Barrick, J. D., Diskin, G. S., Huey, L. G., Fried, A., Cohen, R. C., Heikes, B., Wennberg, P. O., Singh, H. B., Blake, D. R., and Shetter, R. E.: HO_x chemistry during INTEX-A 2004: observation, model calculation, and comparison with previous studies, *J. Geophys. Res.*, 113, D05310, doi:10.1029/2007JD009166, 2008.
- Ridley, B. A., Grahek, F. E., and Walega, J. G.: A small, high-sensitivity, medium-response ozone detector suitable for measurements from light aircraft, *J. Atmos. Ocean. Tech.*, 9, 142–148, doi:10.1175/1520-0426(1992)009<0142:ASHSMR>2.0.CO;2, 1992.
- Roberts, J. M. and Bertman, S. B.: The thermal decomposition of peroxyacetic nitric anhydride (PAN) and peroxyacetic nitric anhydride (MPAN), *Int. J. Chem. Kin.*, 24, 297–307, doi:10.1002/kin.550240307, 1992.
- Rohrer, F. and Brüning, D.: Surface NO and NO₂ mixing ratios measured between 30° N and 30° S in the Atlantic region, *J. Atmos. Chem.*, 15, 253–267, 1992.
- Rohrer, F., Bohn, B., Brauers, T., Brüning, D., Johnen, F.-J., Wahner, A., and Kleffmann, J.: Characterisation of the photolytic HONO-source in the atmosphere simulation chamber SAPHIR, *Atmos. Chem. Phys.*, 5, 2189–2201, doi:10.5194/acp-5-2189-2005, 2005.

- Saunders, S. M., Jenkin, M. E., Derwent, R. G., and Pilling, M. J.: Protocol for the development of the Master Chemical Mechanism, MCM v3 (Part A): tropospheric degradation of non-aromatic volatile organic compounds, *Atmos. Chem. Phys.*, 3, 161–180, doi:10.5194/acp-3-161-2003, 2003.
- Schlosser, E., Bohn, B., Brauers, T., Dorn, H.-P., Fuchs, H., Häsel, R., Hofzumahaus, A., Holland, F., Rohrer, F., Rupp, L. O., Siese, M., Tillmann, R., and Wahner, A.: Intercomparison of two hydroxyl radical measurement techniques at the atmosphere simulation chamber SAPHIR, *J. Atmos. Chem.*, 56, 187–205, doi:10.1007/s10874-006-9049-3, 2007.
- Schlosser, E., Brauers, T., Dorn, H.-P., Fuchs, H., Häsel, R., Hofzumahaus, A., Holland, F., Wahner, A., Kanaya, Y., Kajii, Y., Miyamoto, K., Nishida, S., Watanabe, K., Yoshino, A., Kubistin, D., Martinez, M., Rudolf, M., Harder, H., Berresheim, H., Elste, T., Plass-Dülmer, C., Stange, G., and Schurath, U.: Technical Note: Formal blind intercomparison of OH measurements: results from the international campaign HOxComp, *Atmos. Chem. Phys.*, 9, 7923–7948, doi:10.5194/acp-9-7923-2009, 2009.
- Stone, D., Evans, M. J., Commane, R., Ingham, T., Floquet, C. F. A., McQuaid, J. B., Brookes, D. M., Monks, P. S., Purvis, R., Hamilton, J. F., Hopkins, J., Lee, J., Lewis, A. C., Stewart, D., Murphy, J. G., Mills, G., Oram, D., Reeves, C. E., and Heard, D. E.: HO_x observations over West Africa during AMMA: impact of isoprene and NO_x, *Atmos. Chem. Phys.*, 10, 9415–9429, doi:10.5194/acp-10-9415-2010, 2010.
- Tan, D., Faloon, I., Simpas, J. B., Brune, W., Shepson, P. B., Couch, T. L., Summer, A. L., Carroll, M. A., Thornberry, T., Apel, E., Riemer, D., and Stockwell, W.: HO_x budget in a deciduous forest: results from the PROPHET summer 1998 campaign, *J. Geophys. Res.*, 106, 24407–24427, 2001.
- Taraborrelli, D., Lawrence, M. G., Crowley, J. N., Dillon, T. J., Gromov, S., Grosz, C. B. M., Vereecken, L., and Lelieveld, J.: Hydroxyl radical buffered by isoprene oxidation over tropical forests, *Nat. Geosci.*, 5, 190–193, doi:10.1038/ngeo1405, 2012.
- Tuazon, E. C. and Atkinson, R.: A product study of the gas-phase reaction of methacrolein with the OH radical in the presence of NO_x, *Int. J. Chem. Kin.*, 22, 591–602, doi:10.1002/kin.550220604, 1990.
- Volz-Thomas, A., Xueref, I., and Schmitt, R.: An automatic gas chromatograph and calibration system for ambient measurements of PAN and PPN, *Environ. Sci. Pollut. Res.*, 4, 72–76, 2002.
- Whalley, L. K., Edwards, P. M., Furneaux, K. L., Goddard, A., Ingham, T., Evans, M. J., Stone, D., Hopkins, J. R., Jones, C. E., Karunaharan, A., Lee, J. D., Lewis, A. C., Monks, P. S., Moller, S. J., and Heard, D. E.: Quantifying the magnitude of a missing hydroxyl radical source in a tropical rainforest, *Atmos. Chem. Phys.*, 11, 7223–7233, doi:10.5194/acp-11-7223-2011, 2011.
- Wolfe, G. M., Thornton, J. A., Bouvier-Brown, N. C., Goldstein, A. H., Park, J.-H., McKay, M., Matross, D. M., Mao, J., Brune, W. H., LaFranchi, B. W., Browne, E. C., Min, K.-E., Wooldridge, P. J., Cohen, R. C., Crounse, J. D., Faloon, I. C., Gilman, J. B., Kuster, W. C., de Gouw, J. A., Huisman, A., and Keutsch, F. N.: The Chemistry of Atmosphere-Forest Exchange (CAFE) Model – Part 2: Application to BEARPEX-2007 observations, *Atmos. Chem. Phys.*, 11, 1269–1294, doi:10.5194/acp-11-1269-2011, 2011.
- Wolfe, G. M., Crounse, J. D., Parrish, J. D., St. Clair, J. M., Beaver, M. R., Paulot, F., Yoon, T., Wennberg, P. O., and Keutsch, F. N.: Photolysis, OH reactivity and ozone reactivity of a proxy for isoprene-derived hydroperoxyenals, *Phys. Chem. Chem. Phys.*, 14, 7276–7286, doi:10.1039/C2CP40388A, 2012.